MINISTRY OF EDUCATION AND TRAINING

VIETNAM ACADEMY OF SCIENCE & TECHNOLOGY

GRADUATE UNIVERSITY OF SCIENCE AND TECHNOLOGY

Pham Van Hao

SYNTHESIS OF ELECTROCHEMICALLY GRAPHENE NANOSHEETS FOR APPLICATION AS ADDITIONAL MATERIAL IN ENVIRONMENTAL TREATMENT

SUMMARY OF DISSERTATION ON ELECTRONIC MATERIALS

Code: 9 44 01 23

HA NOI – 2024

The work was completed at:

GRADUATE UNIVERSITY OF SCIENCE AND TECHNOLOGY - VIETNAM ACADEMY OF SCIENCE AND TECHNOLOGY

Science instructor:

1. Assoc. Prof. Dang Van Thanh, Thai Nguyen University of Medicine and Pharmacy
2. Ph. D. Phan Ngoc Hong, Center for High Technology Development - Vietnam Academy of Science and Technology.

Referee 1: .....

Referee 2: .....

Referee 3: .....

The dissertation will be examined by Examination Board of Graduate University of Science and Technology, Vietnam Academy of Science and Technology at…….. (time, date……)

The dissertation can be found at:

1. Graduate University of Science and Technology Library
2. National Library of Vietnam

BEGINNING

Graphene is a monolayer carbon network with a honeycomb structure, with sp^2 hybridized carbon atoms. After obtained the Nobel Prize in 2004, Graphene materials has attracted great interest in academic research as well as applied research due to special physical and chemical properties such as high mechanical strength, outstanding thermal and electrical conductivity, chemical stability and high specific surface area. Many different techniques have been developed to fabricate graphene such as mechanical excision, liquid phase excision (LPE), electrochemical excision, CVD chemical vapor deposition, physical vapor deposition, Epitaxy... Among the aforementioned methods, electrochemical exfoliation is widely used to manufacture graphene materials for environmental treatment and energy storage applications due to advantages such as simple one-step process, low cost, environmental friendliness and automation ability to expand manufacturing scale. The principle of this technique is based on the exfoliation of graphite to form layered graphene that occurs on the positive, negative or both electrodes depending on the control method in the electrochemical reaction vessel. Due to the simple advantage of building an electrochemical system, electrolyte-containing water is readily available, easy to use, and cost-effective, the anodizing technique (used for graphene extraction on the anode) is often used in graphene production. The limitation of this technique is that the obtained material contains many structural defects and oxygen-containing functional groups due to the oxidation reaction. However, this is also an advantage of the technique from an application perspective as it can be used as a composite material or for environmental remediation, as the oxygen-containing functional groups allow the material to be modified or combined with other materials through these functional groups or interact with pollutants. In particularly, for applications in treating wastewater being polluted by dyes or heavy metal ions, the adsorption method is used due to oxygen-containing groups that easily disperse in water and have a strong affinity for positively charged pollutants such as cationic dyes or heavy metal ions. However, most current research is limited to small-scale laboratory experiments. Scaling up the manufacturing process faces many technical challenges such as controlling the supply of electrolytes, voltage stability, heat stability, and arranging electrodes for efficient mass transfer and automation. Therefore, finding a method to electrochemically produce graphene on a large scale, environmentally friendly, with simple equipment and operation is still a truly open question that needs to be explored and resolved.

In Vietnam, graphene and graphene-based composite materials are being researched at various institutions such as the Vietnam National University in Hanoi, the Institute of Materials Science, Hanoi University of Science and Technology, and the University of Science, Ho Chi Minh City. In particularly, the researches relating to the use of graphene-based materials as adsorbents for treating pollutants such as methylene blue dye and metal ions like Cr and As has recently gained a lot of attention with the results which are being published in reputation journals. In general, the research groups commonly use two main methods: chemical vapor deposition (CVD) or producing graphene by reducing GO which obtains from graphite oxide being synthesized via the chemical oxidation routes of Brodie (1859), Hummers and Offeman (1958). In general, the research groups often use two main methods, chemical vapor deposition (CVD) or obtaining graphene by reducing GO from graphite oxide. This graphite oxide is usually synthesized by the chemical oxidation methods of Brodie (1859), Hummers, and Offeman (1958). However, the CVD method requires high technical expertise, expensive equipment, and strict working conditions while the yield is low, so it is only suitable for in-depth

research or applications, such as electronic device fabrication. The methods of production via chemical oxidation pathways often use solvents with strong oxidative properties and toxicity. The excess solvent after production needs to be treated, leading to high costs or secondary environmental pollution. In addition, these approaches are typically limited to experimental scale and are not suitable for practical applications, especially for large-scale, environmentally friendly production processes with reasonable costs. Therefore, it is essential to research and develop new methods of graphene production to address these challenges.

Starting from addressing the above-mentioned issues, combined with the laboratory conditions and research requirements, I chose to implement the dissertation topic "Research on the fabrication of graphene materials using electrochemical methods for environmental remediation applications".

Thesis objective: The research developed the technique of electrochemical exfoliation of traditional positive electrodes to produce a multi-layer graphene material with high automatic capability and environmental friendliness. The resulted material has the potential to be used as an adsorbent for treating MB dye and As metal in water environments.

To realize the above goal, the following specific research works have been implemented:

- One-step fabrication of multilayer graphene material containing rich in oxygen functional groups on the surface from graphite on a gram scale.

- Investigate the morphology and structure of the obtained material.

- Explain the mechanism of creating materials and establish the optimal process to make samples, suitable to the need for materials to adsorb methylene blue and arsenic in water.

- Conduct the batch adsorption experiments to test the adsorption capacity of the produced graphene materials and study the adsorption mechanism of methylene blue and arsenic in water.

Research subject: Graphene material, methylene blue dye, arsenic in aqueous solution in the laboratory.

Research method: The results of the dissertation are obtained through experimental methods. Graphene material is fabricated in a one-step process using electrochemical methods. The structure and morphology are analyzed and evaluated based on measurements from scanning electron microscopy (SEM), transmission electron microscopy (TEM), atomic force microscopy (AFM), X-ray photoelectron spectroscopy (XPS), X-ray diffraction (XRD), and Raman spectroscopy. From the obtained adsorption experimental results, adsorption efficiency, maximum adsorption capacity are calculated, adsorption mechanism is explained, and the adsorption isotherm and kinetic model are identified to adjust the properties of the graphene material to improve its adsorption capacity.

Dissertation structure: The thesis is divided into four chapters.

Chapter 1. Overview

Chapter 2. Experimental methods

Chapter 3. Research results on the electrochemical fabrication of graphene

Chapter 4. Adsorption capacity testing of graphene materials fabricated by electrochemical methods.

Scientific and practical significance

Scientific significance

- Mastering the electrochemical technology for producing gram-scale graphene under normal conditions.

- The composition of the graphene material (functional groups containing oxygen) can be changed to suit the application orientation as an adsorbent material.

Practical significance

- Graphene material is manufactured, in one step, using an environmentally friendly neutral electrolyte, under normal conditions with a self-installed equipment system right in the laboratory.
- The output at the gram/hour scale and the oxygen-rich structural composition of the graphene material are suitable for the application orientation of adsorbing substances in water environments.
- Test results applied as adsorbent materials show that MGSs and O-MGSs materials have good adsorption capacity.

Some new results achieved by the thesis:

- By using one-step electrochemical method with high automation capabilities, we have successfully fabricated and clearly explained the mechanism of the exfoliation multilayer graphene material from graphite rods. The resulting graphene material has a thickness of about 3.5 nm - 4 nm and is rich in oxygen-containing functional groups (C-OH, C-O, C=O) on the surface.
- We have built a multi-electrode electrochemical system which is capable of manufacturing graphene materials at the g/h scale. The amount of graphene material obtained after each 60-minute reaction is about 10 g.
- Graphene material has been applied to investigate the adsorption capacity of methylene blue (MB) and arsenic in water. Research results show that the fabricated graphene material has maximum adsorption capacity with MB reaching 476.19 mg/g and Arsenic reaching 93.45 mg/g.

CHAPTER I. OVERVIEW

Chapter 1 includes 37 pages presenting an overview of graphene materials and methods for creating graphene. In particular, we present in detail the electrochemical method to fabricate graphene material, electrochemical techniques and factors affecting the morphology and structure of graphene material through research conducted by our group and around the world, the properties and applications of graphene in environmental treatment. Applications of graphene materials in environmental treatment are often mentioned with three main applications: filter membranes, photocatalytic composite materials and adsorbent materials. The electrochemical method has the advantage of one-step manufacturing under normal conditions, is simple, environmentally friendly, and has the ability to automate expanding production to meet the requirements of adsorption applications, so it has attracted a lot of attention. The analysis in this chapter is the basis for us to research and develop improvements in traditional electrochemical methods to manufacture one-step graphene for use as an adsorbent in environmental treatment.

CHAPTER 2. EXPERIMENTAL METHODS

Chapter 2 is presented in 12 pages with the following main contents:

2.1. Chemicals and laboratory equipments

2.2. Experimental procedure for manufacturing graphene by electrochemical method.

2.3 Material characteristic measurements: scanning electron microscope (SEM), transmission electron microscope (TEM), atomic force microscope (AFM), X-ray photoelectron spectroscopy (XPS) measurements, X-ray diffraction (XRD), raman scattering spectrum.

2.4 Procedure for determining the isoelectric point of a material.

2.5 Testing application as adsorbent material: methylene blue dye and arsenic in water environment using static adsorption method, the concentration of methylene blue and arsenic was determined using UV-vis spectrophotometer and Atomic absorption spectroscopy.

CHAPTER 3. RESEARCH RESULTS OF GRAPHENE MATERIAL MANUFACTURING BY ELECTROCHEMICAL METHOD

This chapter presents the results of: (i) the study of graphene material synthesis (GSs) by electrochemical method on a two-electrode system, the factors affecting the yield, structure of graphene material; (ii) the study of multi-electrode electrochemical system to scale up the production of graphene material and functionalize the graphene material (O-MGSs) to enhance the adsorption capacity of the material.

3.1 Graphene synthesis using anodic electrochemical technique

3.1.1 The influence of synthesis conditions on the properties of graphene.

As mentioned and analyzed in the overview, the properties of graphene material synthesized by electrochemical method depend heavily on experimental conditions such as working electrode, electrolyte concentration, applied potential, electrode quality, electrolysis temperature, synthesis time, etc. Therefore, it is necessary to study and find the optimal experimental input parameters to obtain graphene with the desired morphology and structure suitable for the intended applications. Based on literature analysis and experimental process, we found that the electrolyte and applied potential have a significant impact on the yield and structure of the obtained material. In particular, graphene with functional groups containing oxygen is favorable for the targeted adsorption process. Therefore, in this section, we synthesized graphene materials using different electrolytes and found the appropriate applied potential for each experiment to control the morphology and structure of graphene material to serve as an adsorbent material for environmental treatment applications.

Table 3.1 Results of investigating the efficiency of manufacturing graphene materials by electrochemical methods using different electrolytes.

Electrolyte	Electrolyte concentration (%)	Sample	Voltage (V)	Time (minutes)	Mass of material obtained (g)
NH_4NO_3	5	GSs-n	+ 15	30	0,12
KOH	5	GSs-k	+ 15	30	0,07
$(NH_4)_2SO_4$	5	GSs-s	+ 15	30	0,62
KOH+$(NH_4)_2SO_4$	5	GSs-ks	+ 15	30	0,51

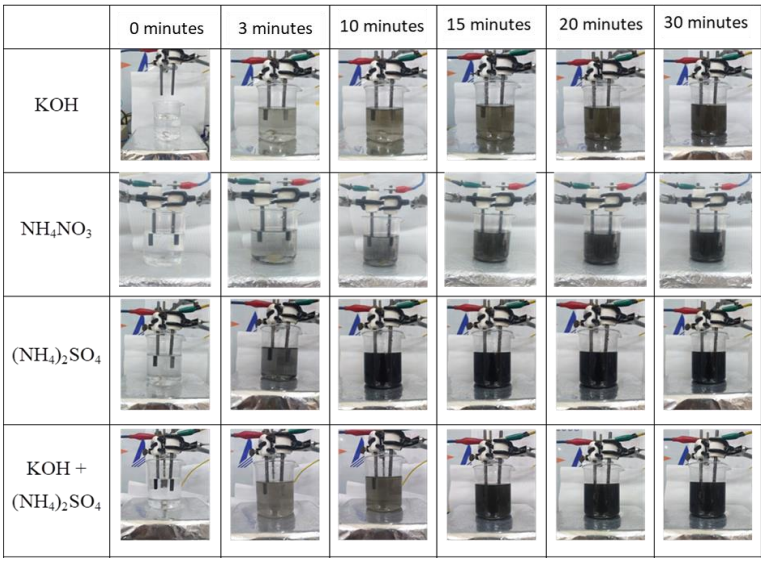

Figure 3.1 Photograph of the electrochemical process of manufacturing graphene with different electrolytes.

3.1.1.1 Electrolyte

Graphene materials manufacturing experiments using anodic electrochemical technique with different electrolytes at an applied potential of +15 V and an electrolysis time of 30 minutes and the results is presented in Table 3.1 The experimental results show that the efficiency of graphene material synthesis depends greatly on the type

of electrolyte used for the electrochemical system, as shown in Table 3.1, where the $(NH_4)_2SO_4$ solution as the electrolyte exhibited the highest efficiency in terms of the yield of the obtained material by mass.

The differences in the surface morphology of graphene materials synthesized using electrochemical techniques with different electrolytes are shown through SEM images (Figure 3.2). It can be seen that the initial graphite material (small image in Figure 3.2a) has a thick, stacked-layer structure, which transformed into a thin-layer form in all four obtained materials using the four different electrolytes. Among them, the material obtained using the electrolyte mixture of $(NH_4)_2SO_4$ and KOH exhibited a clearer thin-layer characteristic compared to the use of the other electrolytes.

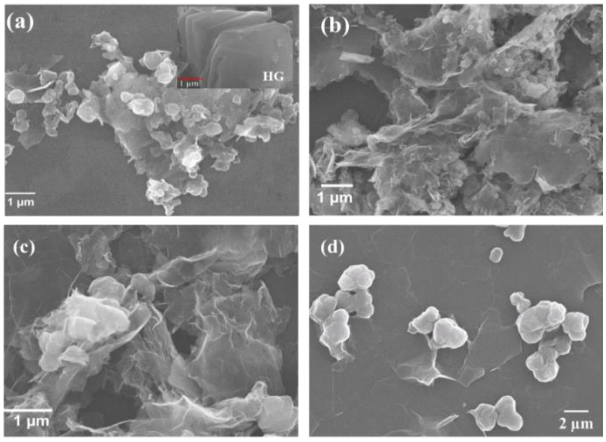

Figure 3.2 SEM images of graphene materials using different types of electrolyte solutions (a) KOH, (b) $(NH_4)_2SO_4$, (c) $(NH_4)_2SO_4$ + KOH, (d) NH_4NO_3, HG (inset) is a graphite material.

Raman spectroscopy is an effective tool for quickly and accurately assessing the characteristics of graphene. Typically, Graphene's raman spectrum has three characteristic peaks: the G peak observed at 1582 cm^{-1}, present in both graphene and graphite, is characteristic of the vibrational mode of the sp^2 hybridized carbon atoms in the two-dimensional hexagonal lattice of graphene; the second peak is the D peak appearing around 1350 cm^{-1}, characteristic of lattice defects and sp3 hybridization presents in the graphene material. The D peak is typically very weak for high-quality graphite and graphene with few defects and oxygen-containing functional groups. If the D band is significant, it indicates that the material has a lot of crystal lattice defects or contains many heterophases. The intensity ratio of the D and G peaks (ID/IG) tells us the degree of defects or disorder in the structure of graphene; the third peak is the 2D peak observed at 2700 cm-1, which is the result of a two-phonon oscillation process. The 2D peak is symmetric for graphene and asymmetric for graphite

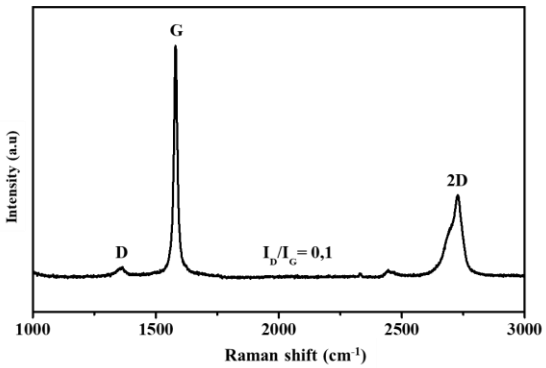

Figure 3.3. Raman spectrum of graphite.

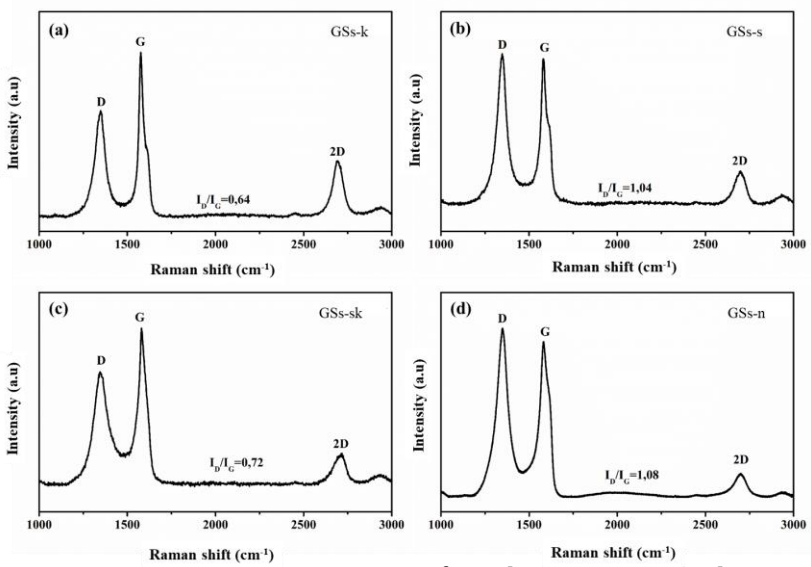

Figure 3.4. Raman spectrum of graphene prepared with electrolyte solutions (a) KOH, (b) $(NH_4)_2SO_4$, (c) KOH + $(NH_4)_2SO_4$, (d) NH_4NO_3.

at a position with a larger wavelength shift than 2700 cm-1 [140]. Therefore, the GSs-n, GSs-sk, GSs-n, and GSs-k samples were analyzed by Raman spectroscopy to quickly obtain information on the influence of the electrolyte on the composite samples, combined with SEM to obtain optimal conditions. As indicated in the Raman spectra results (Figure 3.4), all the samples obtained have a symmetric 2D peak characteristic of thin-layer materials, unlike the asymmetric 2D peak in the Raman spectra of graphite materials (Figure 3.3). In addition, the intensity ratio of the D peak to the G peak (I_D/I_G) of the graphene material samples obtained has values of 0.64, 1.04, 0.72, and 1.08, respectively, for the electrolytes KOH, $(NH_4)_2SO_4$, KOH + $(NH_4)_2SO_4$, NH_4NO_3. These I_D/I_G ratios have different values, indicating that the level of structural damage in the material varies when using different electrolytes.

The composition of the graphite and GSs-s, GSs-sk, GSs-n, and GSs-k samples was clarified by XPS spectral analysis, as shown in Figures 3.5 and 3.6. It can be clearly seen that the high-quality graphite has low oxygen content (the presence of oxygen in graphite may be due to the sample preparation process), while the graphene materials show more oxygen presence. Specifically, in the GSs-s, GSs-sk, and GSs-n samples, there are peaks appearing at energy positions of 284.5, 284.8, 285.4, 286.5, 287.6, and 288.8 eV, corresponding to the bonds of carbon atoms with carbon and with oxygen, namely C=C, C-C, C-OH, C-O, C=O, C(O)OH [141]. The remaining graphene material sample using KOH as the electrolyte, GSs-k, does not show peaks corresponding to the functional groups C=O and C(O)OH. This could be due to the oxidation reactions on the positive electrode being inhibited in the electrolyte solution containing only KOH. Combining these results with the Raman measurements, we conclude that the cause of defects in the graphene material's structure is the attachment of oxygen-containing groups to the graphene sample. The varying degrees of oxidation in the electrolyte solutions used in the electrochemical system lead to different levels of electrode oxidation. This differential oxidation results in structural damage, varying levels of additional oxygen-containing functional groups, and, consequently, different I_D/I_G ratios.

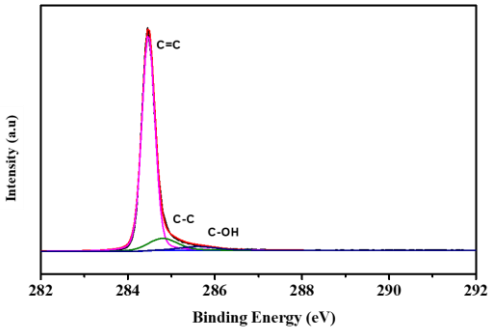

Figure 3.5. XPS spectrum of graphite.

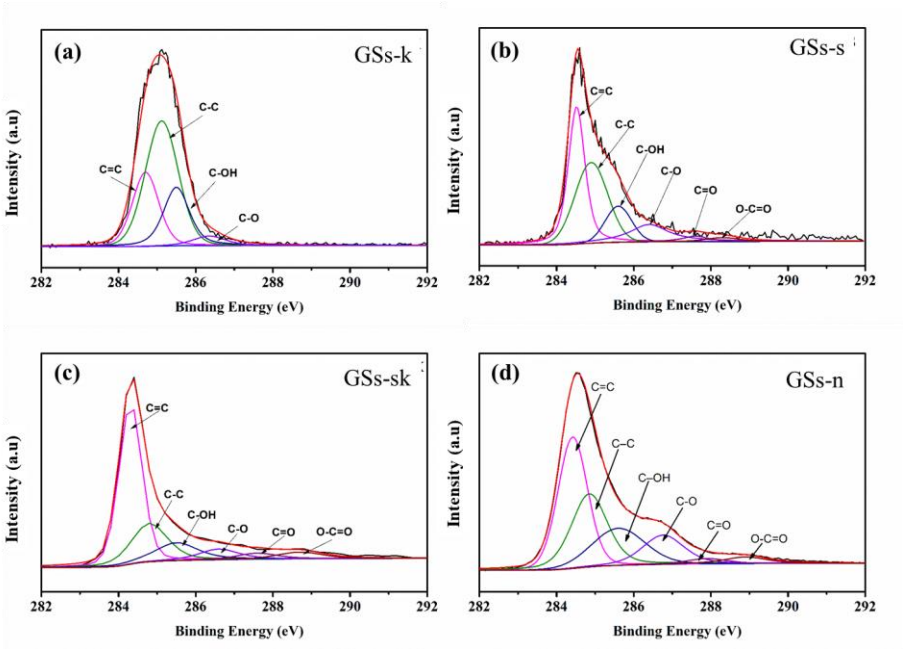

Figure 3.6. XPS C1s spectrum of graphene material fabricated with electrolyte solution (a) KOH, (b) $(NH_4)_2SO_4$, (c) KOH + $(NH_4)_2SO_4$, (d) NH_4NO_3.

Thus, through the results of this research, we can see that electrolytes have a big impact on the properties of the graphene material obtained after the electrochemical process.

Specifically, the electrolyte containing KOH has low defects and negligibly low yields; the solution containing NH_4NO_3 has the highest defect level and oxygen content in the sample due to its strongest oxidative properties. The solution containing $(NH_4)_2SO_4$ is the most efficient in producing graphene materials separated from the electrode and has great potential for large-scale material fabrication, which is the focus of our research.

However, the rapid exfoliation of the graphene materials from the graphite electrode in the electrolytic solution containing $(NH_4)_2SO_4$ or NH_4NO_3 leads to the exfoliation of even thick graphite pieces, reduces the uniformity of the material and decrease the effectiveness when used as an adsorbent material. Therefore, to harmonize the factors, their mixture is a reasonable choice for the purpose of application as an adsorbent material.

The effect of $(NH_4)_2SO_4$ concentration in the electrolyte solution on the structure and yield of the material was also studied. $(NH_4)_2SO_4$ solution was used at concentrations from 1 to 10 % as shown in Table 3.2 and was quickly evaluated via Raman spectrum (Figure 3.7).

It can be seen that as the concentration of $(NH_4)_2SO_4$ increases, the intensity of peak D and

Table 3.2 The amount of material obtained depends on the concentration of $(NH_4)_2SO_4$

Concentration $(NH_4)_2SO_4$ (%)	Voltage (V)	Sample	Mass of material obtained (g)
1,0	15	GSs-s-1	-
2,5	15	GSs-s-2,5	0,16
5,0	15	GSs-s-5,0	0,62
7,5	15	GSs-s-7,5	0,68
10	15	GSs-s-10	0,71

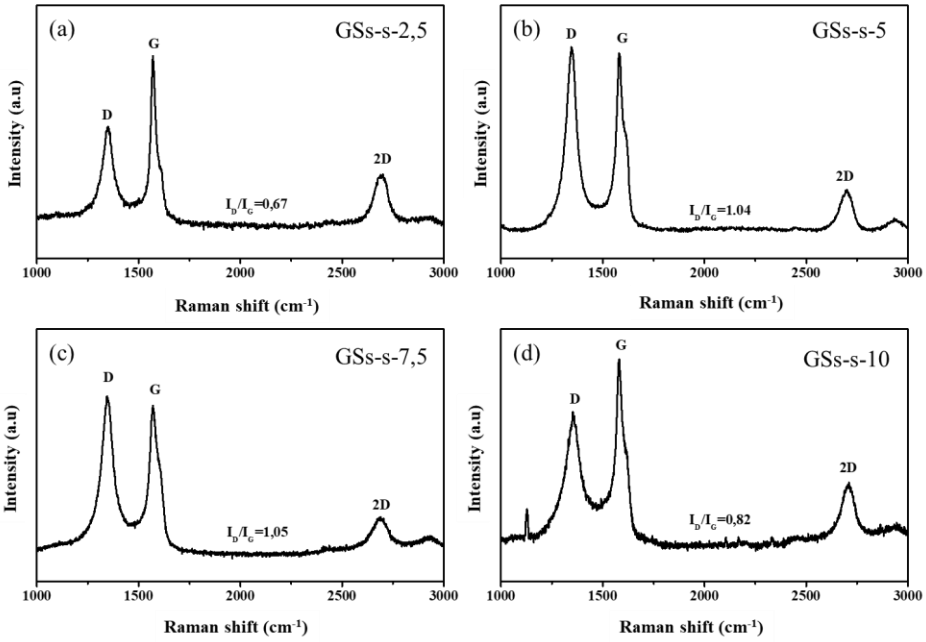

Figure 3.7. Raman spectra of graphene materials fabricated with $(NH_4)_2SO_4$ electrical solution at concentrations of (a) 2.5 %, (b) 5%, (c) 7.5 %, (d) 10 %.

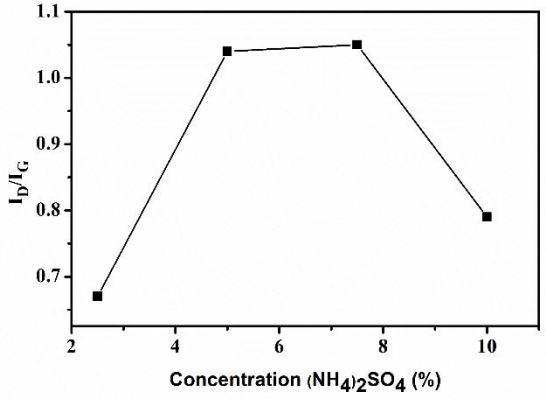

Figure 3.8. The intensity ratio of the D and G peaks in the Raman spectrum of graphene material at $(NH_4)_2SO_4$ concentration.

I_D/I_G ratio increase. However, this increase is not linear (as in Figure 3.8), as the ratio I_D/I_G decreases when the concentration increases. We believe that as the concentration of $(NH_4)_2SO_4$ increases, the water content in the solution decreases, hindering the approach of hydroxyl groups to the positive electrode, thereby reducing the oxidation of the electrode leading to a decrease in the I_D/I_G ratio of the material. Therefore, we conclude that $(NH_4)_2SO_4$ in a solution with a concentration of 5% is suitable for electrochemical graphene fabrication.

3.1.1.2 Voltage

In addition to the electrolyte, the polarizing voltage also affects the mass and structural composition of the fabricated material. Therefore, studying the influence of the voltage on the efficiency and formation of oxygen-containing functional groups in graphene materials allows for adjustment of the fabrication conditions to obtain the desired material. Table 3.3 presents the results of the dependence of the mass of the obtained material on the voltage applied to the two electrodes. This experiment was conducted with a voltage ranging from 1V to 20V, a 5% $(NH_4)_2SO_4$ electrolyte solution, and a fabrication time of 30 minutes.

The mass of the obtained graphene material significantly increases with the increase of voltage under the same conditions of fabrication time, electrolyte concentration, and distance

Table 3.3 Dependence of the mass of graphene material obtained on the polarization voltage.

Sample	Voltage (V)	Time (minutes)	Mass of material obtained (g)
GSs-1V	1	30	Negligible
GSs-5V	5	30	0,08
GSs-10V	10	30	0,48
GSs-15V	15	30	0,62
GSs-20V	20	30	0,76

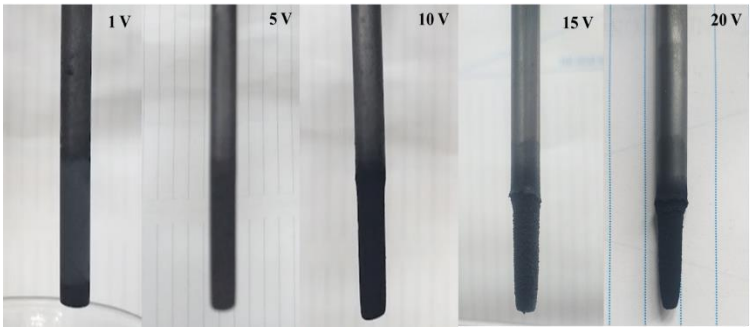

Figure 3.9. photograph of the positive electrode after 30 minutes of electrochemical fabrication of graphene at

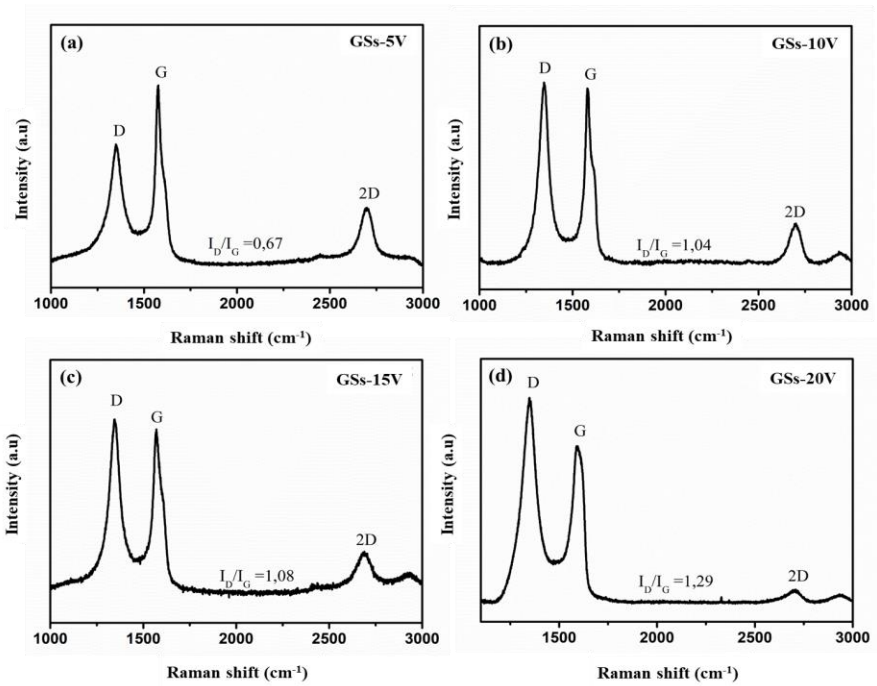

Figure 3.10. Raman spectrum of graphene at voltages (a) 5V, (b) 10V, (c) 15V, (d) 20V.

between the two electrodes. Specifically, at low voltages (1V, 5V), the exfoliation efficiency is insignificant, and the amount of material produced is meager. It may be due to at this voltage value, the current density is small which is not enough to drive the electrochemical reactions generating the gas among the layers in the structure of electrode, so it does not generate enough pressure to exfoliate the layers from graphite to form graphene material. On the contrary, at a higher voltage, the higher current strongly drives the intercalation process and simultaneously promotes the electrochemical reactions generating the gas among the layers of the electrode. These gases exert a strong force to exfoliate the material from the electrode, resulting in a greater overall yield. However, at higher voltages, the exfoliation material process occurs faster, resulting in not only graphene but also thick graphite sheets being obtained, as indicated in reference [44]. Furthermore, we found that the defect level of the material is also found, as observed by the I_D/I_G ratio in the Raman spectra of the obtained materials which increases with the increasing voltage, specifically, the I_D/I_G ratios of the GSs-5V, GSs-10V, GSs-15V, GSs-20V materials are 0.67, 1.04, 1.08, and 1.29, respectively, as shown in Figure 3.10.

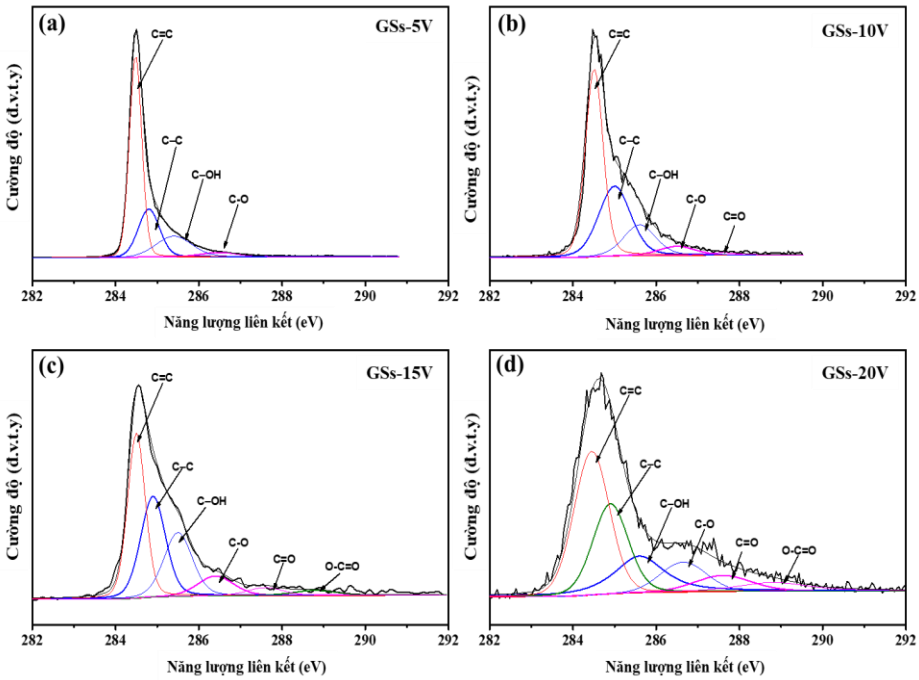

Figure 3.11. XPS spectrum of graphene at voltages (a) 5V, (b) 10V, (c) 15V, (d) 20V.

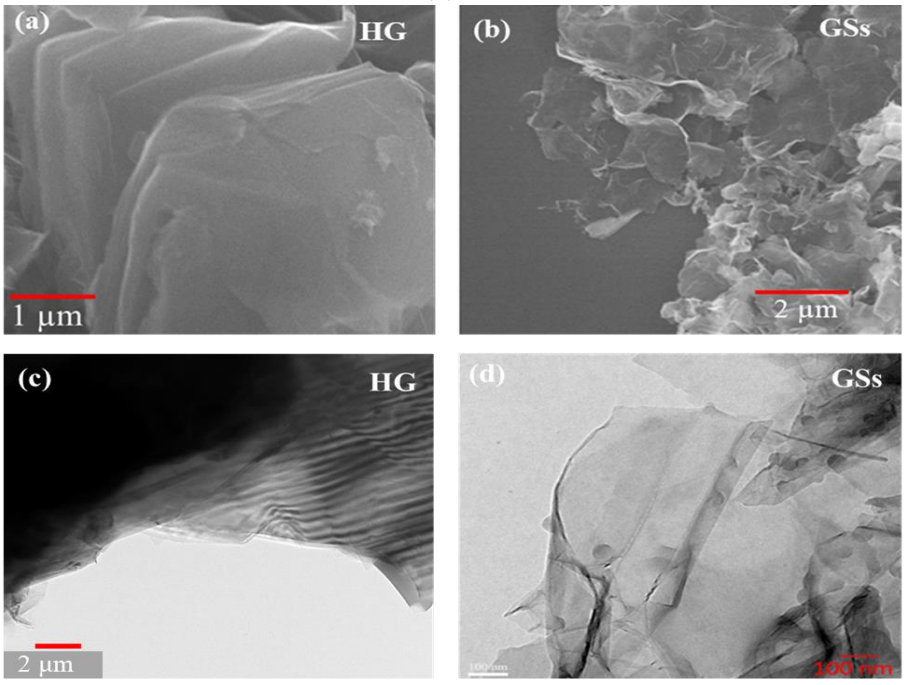

Figure 3.12 SEM images (a) of graphite (HG) and (b) of GSs; TEM images (c) of HG and (d) of GSs

The XPS spectral analysis results help us confirm that the increase of the I_D/I_G ratio in the Raman measurement results (Figure 3.10) is due to the presence of oxygen attached to the material, which disrupts the structure of the graphene material. With these results, we believe that as the polarization voltage increases, the electric field energy between the two electrodes not only makes the ions in the solution fill in more strongly but also promotes the oxidation process at the electrodes, leading to an increase in both the yield and the degree of material oxidation. These results, combined with the Raman measurement results, indicate that the polarization voltage is an important factor in the electrochemical exfoliation process related to the material oxidation. From these experimental results, we conclude that a voltage of 10V is appropriate for the electrochemical process.

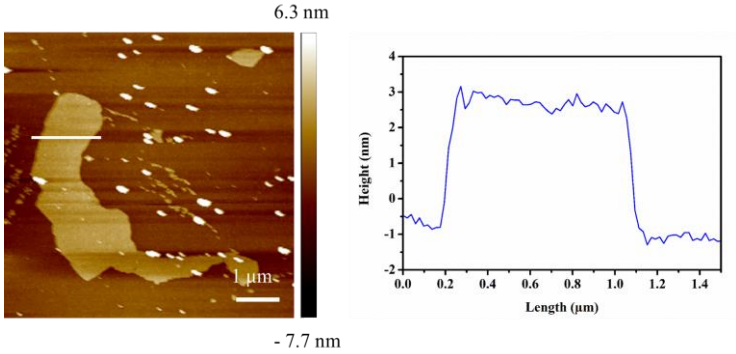

Figure 3.13 AFM image of GSs graphene material

3.1.2 Characteristics of GSs graphene material

From the results of studying the effects of electrolyte and voltage on the efficiency fabrication and structure of graphene materials, we found that fabricating GSs graphene materials at an electric potential of around 10V and using electrolytes containing (NH4)2SO4 and KOH are suitable for adsorption material applications. So, we further assess the specific morphology, structure, and composition of the GSs sample under these conditions. Figure 3.12 shows the SEM and TEM images of the input graphite material (HG) and the graphene material fabricated by the electrochemical method (GSs). It can be seen that HG is in the form of a multi-layered block, with a micrometer size, while GSs exhibits a clearly defined thin layer morphology with wrinkles, folds stacked on top of each other, or rolled up as shown in Figure 3.12 b and d, similar to the results in our previous study [38]. The thickness of the GSs material is 3.5 nm as determined from AFM measurements (Figure 3.13), corresponding to several layers of graphene (from 5 to 7 graphene layers). Raman

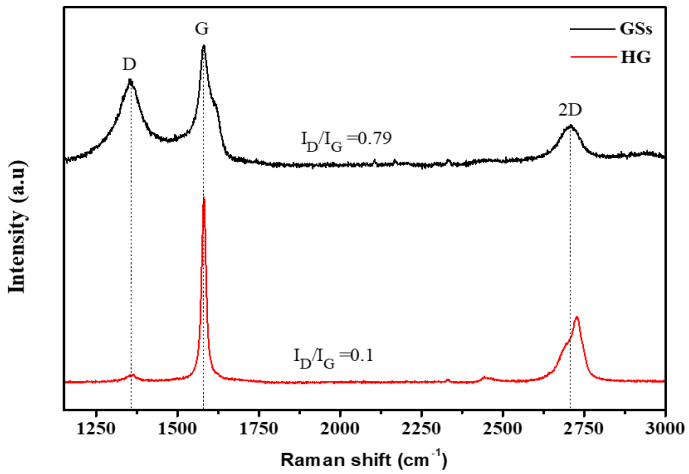

Figure 3.14 Raman spectra of GSs and HG.

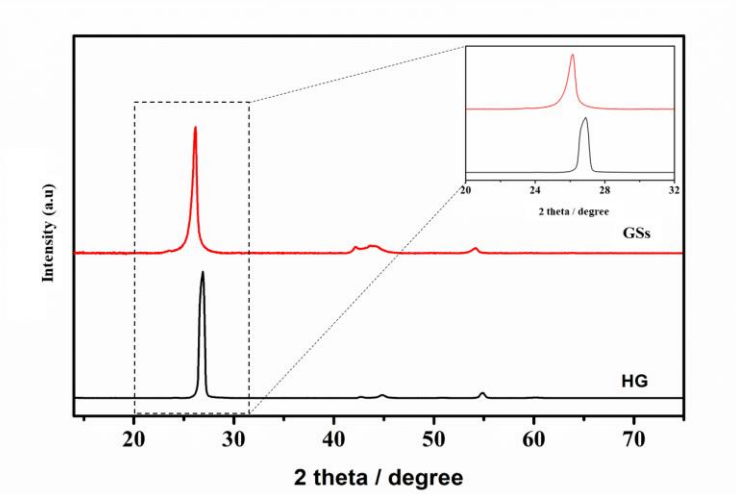

Figure 3.15 XRD patterns of GSs and HG.

measurements of both GSs and HG show 3 characteristic peaks: the D peak at ~1350 cm^{-1}, G at ~1580 cm^{-1}, and the 2D peak at ~2700 cm^{-1} (Figure 3.14). The difference in the symmetrical 2D peak shape in GSs and the asymmetrical shape in HG confirms that GSs are in a thin layer form [140]. As calculated and indicated in Figure 3.14, the I_D/I_G ratio of GSs is 0.79 and of HG is 0.1, showing that the structure of the GSs material is more damaged than the high-quality graphite material HG.

The structural change from a block form to a thin layer of material was further examined through XRD analysis, as shown in Figure 3.15. It can be observed that the HG material exhibits a sharp peak at 26.6 degrees corresponding to the (002) plane, while the GSs material still shows a high-intensity peak at a position shifted to a smaller 2θ value compared to HG at 26.16 degrees and with a broader peak width. The interlayer spacing was calculated based on formula (2.1) and the θ angle from the XRD spectrum, resulting in 0.340 nm for GSs and 0.335 nm for HG, slightly larger than the interlayer spacing in HG due to the oxidation-reduction reactions during the electrochemical process inserting oxygen-containing functional groups between the layers, causing an increase in their distance. This result is consistent with the calculated I_D/I_G ratio of GSs and HG in the Raman spectrum in Figure 3.14.

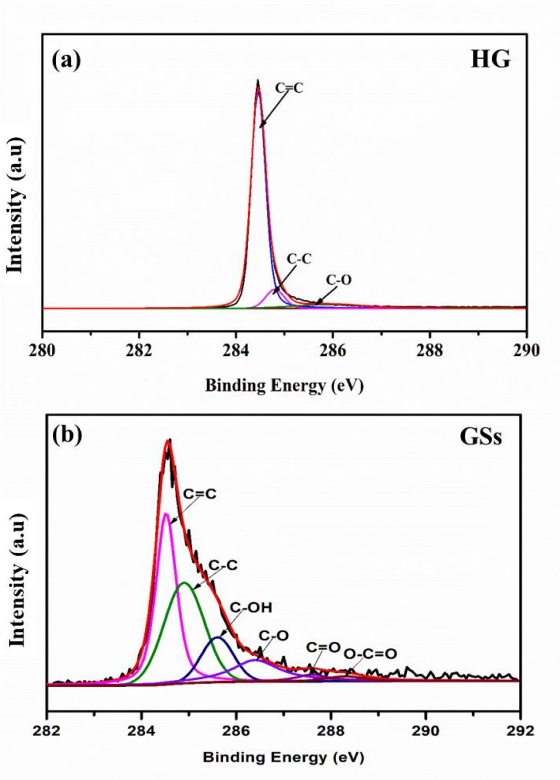

Figure 3.16 XPS C1s spectra of HG (a), of GSs (b).

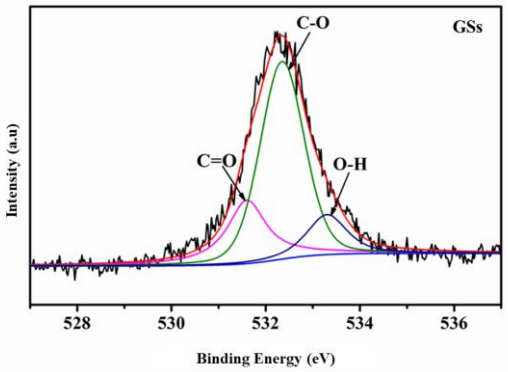

Figure 3.17 XPS O 1s spectrum of GSs.

As explained in the overview, graphite has a layered crystalline structure, with each layer being a sheet of graphene. These layers are held together by weak Van-der-Waals forces. Breaking these Van-der-Waals bonds between the layers causes them to separate into graphene. Essentially, the electric current drives the process of filling the interlayer spaces in the graphite structure with ions from the electrolyte, while also promoting the reactions that decompose these filling substances to generate gas, gradually creating large gas bubbles between the layers that exert significant pressure, pushing the layers apart and weakening the Van der Waals forces between them, ultimately separating them into graphene. During this process, the electrochemical factor also causes oxidation, leading to the degradation of the C=C/sp2 bonds in the crystalline structure and their transformation into C-C/sp3 bonds, or the formation of various functional groups such as C-O, C-OH, C=O, etc., in the fabricated material [139]. To quantitatively determine the composition and the bonds present in the sample, XPS spectroscopy was conducted, and the results are shown in Figure 3.16. In the C1s spectrum of HG (Figure 3.16a), there is a main peak at 284.5 eV representing

the C=C bond, and two minor peaks with weaker intensities at 285.6 eV and 284.8 eV representing the C-C bond and the carbon atom bond with the OH- functional group.

Table 3.4: Calculation results of the bond content in the sample.

Sample	C=C (%)	C–C (%)	C–OH (%)	C–O (%)	C=O (%)
HG	85,11	10,64	4,26	0	0
GSs	44,98	38,55	8,84	5,62	2,01

Figure 3.16 (b) shows the C1s spectrum of the GSs material, similar to the C1s spectrum of HG, with the presence of two main peaks at 284.5 eV and 284.8 eV corresponding to the carbon atoms in the sp2 and sp3 hybridized states. Additionally, this spectrum also shows four additional peaks at 285.6 eV, 286.4 eV, 287.6 eV, and 288.3 eV, corresponding to the carbon atom bonds in the functional groups C-OH, C-O-C, C=O, C(O)OH [141]. Furthermore, the ratio of the C=C/C-C bonds in GSs and HG calculated from the C1s spectrum analysis is 1.07 and 7.8, respectively. This confirms that a significant amount of the sp2 hybridized structures have been broken into sp3 hybridization during the transition from bulk to thin film form. The electrochemical reactions have caused this destruction, resulting in the GSs structure containing numerous network defects or oxygen-containing functional groups, with the specific bonds and their percentages listed in Table 3.4.

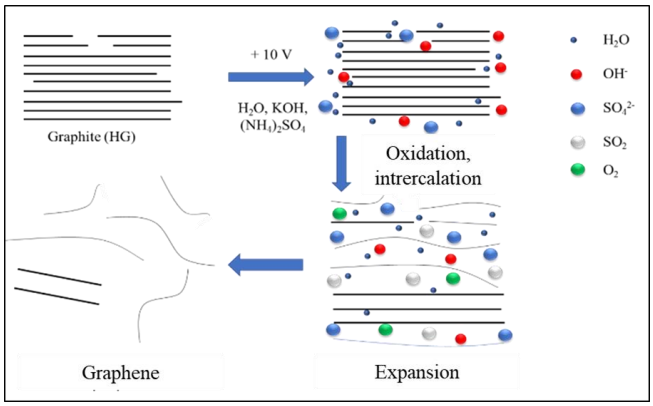

Schematic illustration of the electrochemical exfoliation mechanism

To further clarify these bonds, the O 1s spectrum of GSs was additionally analyzed (Figure 3.17). Three peaks appeared at energy levels of 531.6 eV, 532.3 eV, and 533.3 eV, corresponding to the binding energies of the C=O, C-O, and O-H groups [143]. These results confirm that the GSs sample contains a significant amount of oxygen, consistent with the XPS C1s spectrum of GSs in Figure 3.16.

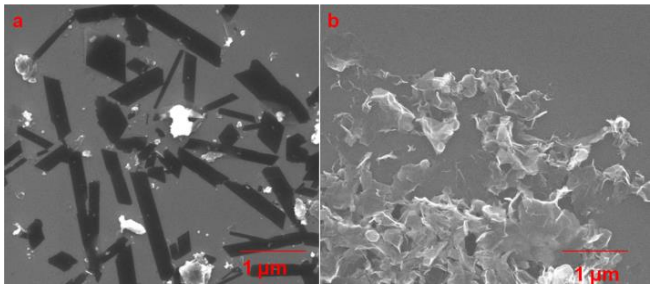

Figure 3.19 SEM images of samples (a) A-GSs and (b) C-GSs.

The mechanism of electrochemical exfoliation of graphene from graphite electrodes (anode electrodes) is explained as in Figure 3.18: first, when voltage is applied to the electrodes, water is reduced at the negative electrode, creating highly active hydroxyl ions (OH-) in the electrolyte solution. Under the influence of the electric field, these OH- ions move towards the positive electrode, causing the oxidation of the graphite electrode. This oxidation initially occurs at the edge positions and defect sites, leading to the expansion of the

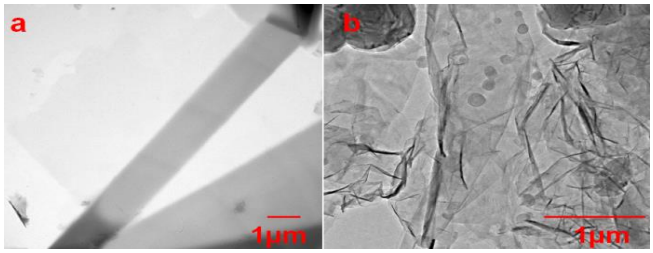

Hình 3.20 TEM images of samples (a) A-GSs and (b) C-GSs.

graphite electrode. This expansion creates favorable conditions for ions in the solution such as OH-, SO42-, and water to intercalate between the graphite layers. Under the influence of the electric field, the oxidation of OH- and the reduction of SO42- anions, and the self-oxidation of water between the layers, produce gases such as SO2, O2 [144, 145]. These gases form bubbles, exerting high pressure on the graphite layers and overcoming the Van der Waals forces, thereby separating these layers into graphene [45].

3.1.3 Graphene fabricated on negative electrode and positive electrode.

The process of making graphene on the positive and negative electrodes is explained as follows: Graphene material is made on the negative electrode using the electrochemical plasma technique (as presented in section 2.2.2) and is denoted as C-GSs. Material A-GSs is made on the positive electrode using the anodic electrochemical technique (as presented in section 2.2.1). In this experiment, both techniques use two high-purity graphite electrodes (99.999% purity), with diameters and lengths of 6mm and 100mm respectively. The electrolyte solution is a mixture of KOH (7.5%) and (NH4)2SO4 (5%) in a 4:1 ratio, and a direct current power source (TES 6220, 60 V/3 A, USA) is used, with a voltage set at 60 V and a current intensity maintained between 1.4 and 1.7 A. The temperature is kept at around 70-80 ºC, and the mixture is stirred at a speed of 250 rpm to ensure the reaction proceeds evenly. The reaction time is approximately 15 minutes.

Polarization not only affects the structure but also the morphology of graphene material. In this section, the research of the thesis aims to compare the properties of materials made on the positive electrode in anodic mode (A-GSs) and the negative electrode (C-GSs). Figures 3.19 and 3.20 are SEM and TEM images of the A-GSs and C-GSs materials respectively. It can be seen that the morphology of the two materials obtained from the two different polarization modes is very distinct, the A-GSs material (Figure 3.19a) is thin sheets, resembling ribbons, while C-GSs (Figure 3.19b) is thin sheets rolled or folded, characteristic of thin layer materials (Figure 3.20b). Using the AFM atomic force microscopy method (Figure 3.21), we

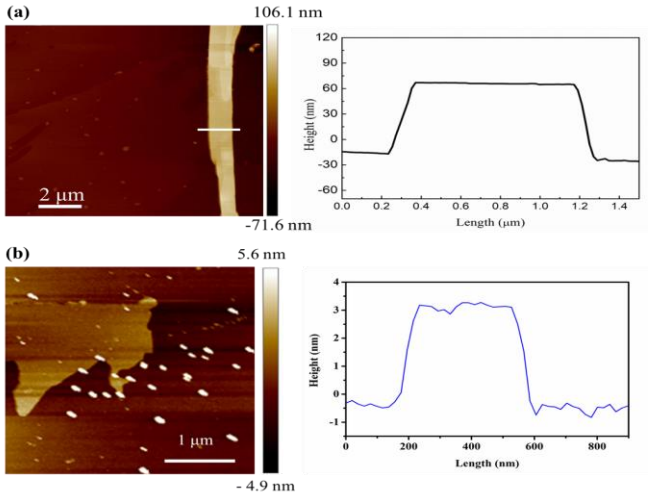

Figure 3.21 AFM images of samples (a) A-GSs and (b) C-GSs.

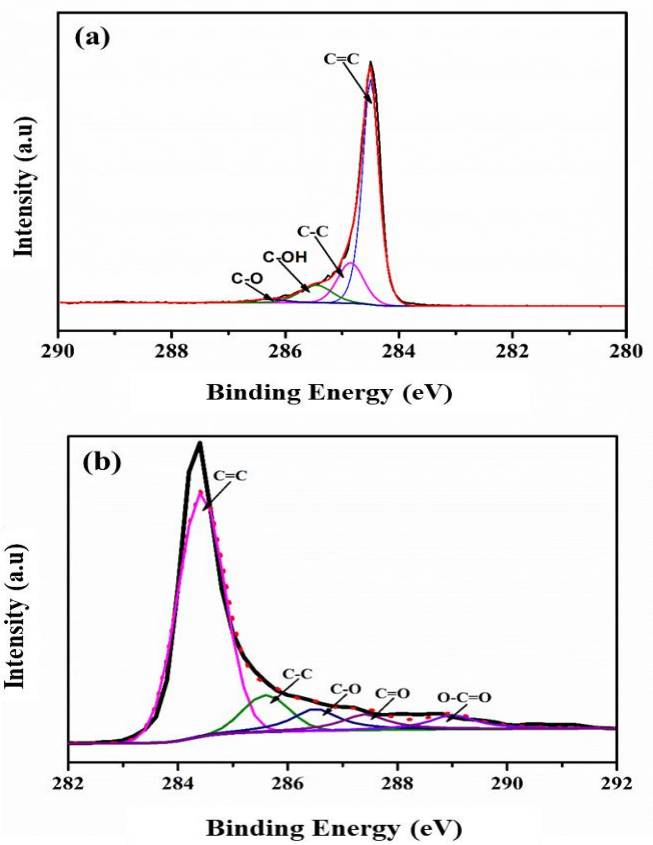

Figure 3.22 XPS spectra of samples (a) A-GSs and (b) C-GSs.

determined the thickness of A-GSs to be 74 nm and the thickness of C-GSs to be 4 nm. As explained the role of the electrolyte in the process of electrochemical graphene synthesis, the size of the ions affects the efficiency of separating graphene material from the graphite electrode. Anions such as SO42- are larger than cations such as OH-, the expansion at the positive electrode occurs faster and more strongly than at the negative electrode. In addition, experiments in both modes were carried out at high voltage (±40-60V), the oxidation-reduction reactions on the electrode occur strongly and release a large amount of gas in a short time causing an explosion. This explosion not only occurs on the surface of the electrode but also occurs within the interlayer space due to the filling of layers between the graphite layers, strong gas-generating reactions also occur. The force of the gas bubble and the force generated from the filling cause expansion, which is the reason for the graphene material at the positive electrode having a higher number of layers than the graphene produced at the negative electrode.

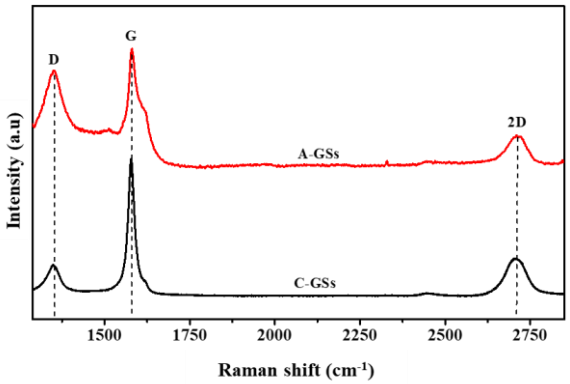

Figure 3.23 Raman spectra of A-GSs and C-GSs

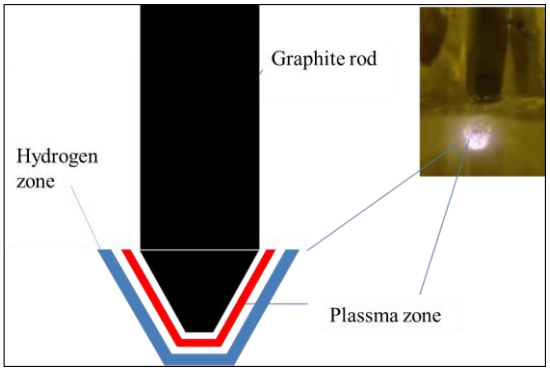

Figure 3.24 Diagram illustrating the hydrogen gas layer at the electrode surface in contact with the electrolyte in the presence of plasma.

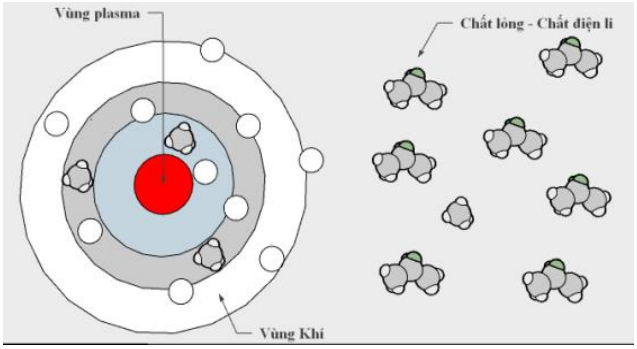

Figure 3.25 Diagram of the structure of the plasma solution region.

The two polarization modes have different effects on the formation of bonds in the sample. As shown in Figure 3.22 and Table 3.5, the A-GSs material has a higher percentage of carbon atoms bonded to oxygen-containing functional groups compared to the C-GSs material. In other words, the sp2 hybridization in the crystal lattice of the C-GSs sample created by plasma electrolyte is less degraded to become more sp3 hybridization. To further confirm this conclusion, Raman spectroscopy measurements were performed to assess defects and the ratio of sp3 hybridization in the samples through the ID/IG ratio. The results in Figure 3.23 and Table 3.6 show that the ID/IG ratio of C-GSs is smaller than the ID/IG ratio of A-GSs, and this result is consistent with the XPS spectroscopy analysis in Figure 3.22.

Table 3.5 Comparison of the amount of linkages in A-GSs and C-GSs.

Sample	C=C (%) ~284,54 eV	C–C (%) ~284,84 eV	C–OH (%) ~285,5 eV	C-O (%) ~286,7 eV	C=O (%) ~287,6 eV
A-GSs	68,19	10,35	9,13	5,76	6,73
C-GSs	69,2	18,7	10,1	2,0	-

Table 3.6 Position of D, G, 2D peaks and ID/IG ratio.

Sample	D peak (cm^{-1})	G peak (cm^{-1})	2D peak (cm^{-1})	I_D/I_G
A-GSs	1348	1575	2705	0,94
C-GSs	1346	1580	2700	0,31

The electrochemical technique pushes the chemical reactions on the electrode to release a strong stream of oxygen gas, enveloping the electrode surface tightly. The gas release combined with the surface oxidation of the electrode in contact with the electrolyte solution leads to the formation of graphite compounds interspersed with functional groups such as hydroxyl, carboxyl... attached to the carbon atoms of C-C/C=C bonds. When interspersed, the bonding force between layers in the graphite compound weakens. The electrochemical agent continues to act, causing these layers to separate into thin graphene layers. The oxidation reactions on the electrode lead to the A-GSs sample containing a lot of oxygen. In the plasma electrochemical mode on the negative electrode, H2 gas molecules are vigorously released around the electrode surface (Figure 3.24), this gas layer prevents oxygen from reacting with the C-C/C=C bonds, thereby reducing the oxidation of the C-C/C=C bonds and thus the percentage of carbon atoms bonded to the oxygen-containing groups in the A-GSs sample is higher than in the C-GSs.

The difference in the amount of oxygen-containing functional groups between A-GSs and C-GSs can be explained as follows: high working potential (± 40 - ± 60V) promotes reduction reactions on the negative electrode releasing a lot of H_2 gas (equation 3.7) and oxidation reactions on the positive electrode releasing a lot of O_2 (equation 3.8).

$$2H^+ + 2e \rightarrow H_2 \qquad 3.7)$$

$$2H_2O \rightarrow O_2 + 4H^+ + 4e \qquad 3.8)$$

Simply, the structure of the plasma region formed on the negative electrode where the sharp tip contacts the electrolyte solution can be modeled as shown in Figure 3.25, although the detailed structure of the plasma so far remains an unexplained phenomenon [146]. On the positive electrode, in anodic mode, the electrochemical process occurs similarly to normal anodic electrochemical mode, with oxidation reactions taking place on the electrode leading to the attachment of oxygen and oxygen-containing functional groups onto graphene [147].

Thus, the polarization mode has different effects on the morphology and structure of graphene materials. Utilizing this property can create a simple way to control the morphology and structure of graphene materials for various applications.

3.2 Mass-production graphene material

3.2.1 Manufacturing graphene material with an electrochemical system of 10 electrode pairs

Using a 10 electrode pair electrochemical system, we were able to manufacture MGSs graphene material, and the amount of graphene material obtained was 10 grams in 60 minutes of electrolysis. It's clear that the material yield obtained in one experiment significantly increased compared to the electrochemical system with each electrode consisting of only 1 graphite rod [148]. In Figure 3.27, it can be seen that as the number of electrodes increases, the obtained material still exhibits similar characteristics to the material manufactured with 2 electrodes, such as being thin and coiled (SEM and TEM images) with a thickness of 4 nm (AFM image),

corresponding to about 4-10 layers of graphene material. To analyze the structural composition, Raman and XPS spectroscopy measurements were carried out. It can be observed that, similar to GSs, the Raman spectrum also has a symmetrical 2D peak around 2700 cm-1 related to the formation of graphene [140]. In particular, the D peak is quite high, as it is usually the result of the electrochemical process related to functional groups or structural defects, introduced into the material during the electrolysis process. Additionally, the XPS C1s spectrum of MGSs (Figure 3.29 b) corresponds to 5 types of bonds at 284.5 eV, which are non-oxidized carbon components (-C = C, sp^2 hybridized carbon atoms), at 285.7 eV for C – C bonds (sp^3 hybridized carbon atoms), at positions 286.3, 288.7, and 287.2 eV for carbon atom bonds in functional groups containing oxygen C-O, C = O, O – C = O (hydroxyl/epoxy, carbonyl, and carboxyl) with the percentage of bonds being 52.18%, 28.53%, 11.28%, 5.74%, and 2.27% respectively [141]. This indicates that the sample still exhibits characteristic features of the composition of electrolytically manufactured graphene material with water as the solvent, containing oxygen groups, and is consistent with the Raman measurement results.

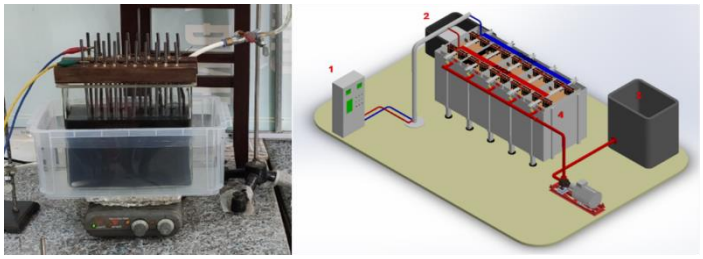

Figure 2.26 Experimental setup diagram for large-scale MGSs graphene material synthesis using 10 pairs of graphite anode/cathode electrodes: (1) power source, (2) product tank, (3) electrolyte solution tank, (4) electrochemical reaction vessel.

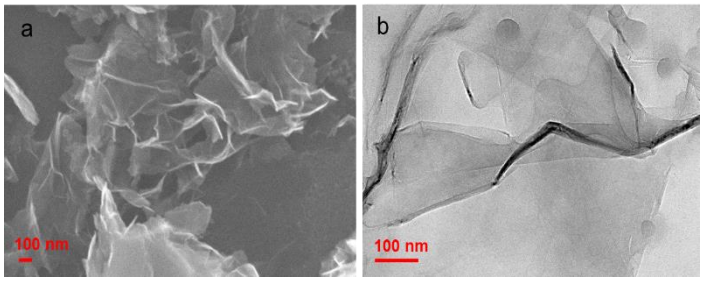

Figure 3.27 SEM (a) and TEM (b) images of MGSs.

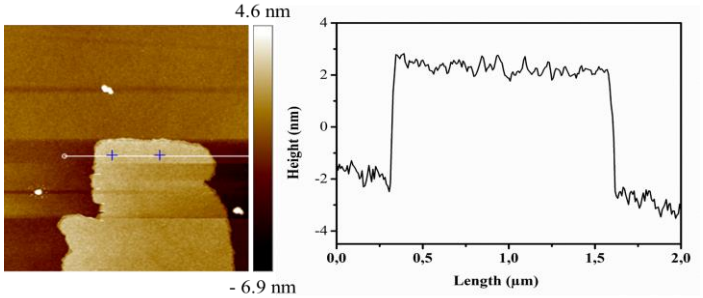

Figure 3.28 AFM image of MGSs and corresponding thickness.

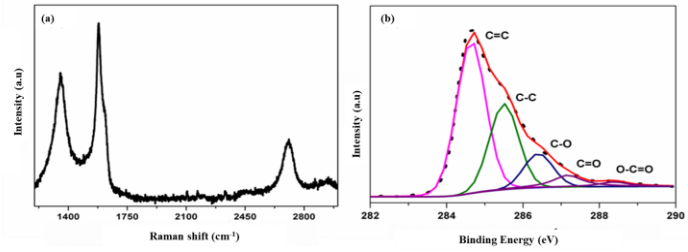

Figure 3.29 Raman spectrum (a) and XPS spectrum of MGSs.

3.2.2 Fabrication of graphene material with an electrochemical system of 10 positive electrodes and 1 negative electrode

Although the amount of graphene material obtained from the multi-electrode electrochemical system increased (gram scale) as desired, new limitations emerged from the experiments. The increased current due to the increased electrode contact area with the solution compared to the two-electrode system. The large current generates intense heat, quickly heating up the electrolyte, making it difficult to maintain the temperature, and the rapid evaporation rate of the electrolyte requires a large amount of replenishment, leading to high costs. Additionally, the graphene extraction process mainly occurs on the positive electrode, allowing us to optimize the number of experimental

electrodes to save costs while still extracting graphene. We also increased the voltage to 30V to enhance the functionalization of oxygen-containing groups on the material surface. Therefore, we reduced the number of graphite rods used as negative electrodes in the electrochemical system to 1 rod and placed it in the middle of the 10 positive electrodes arranged in a circular pattern (Figure 2.30). Reducing the number of graphite rods used as negative electrodes helped us save costs, and arranging them in a circular pattern ensures an even extraction on all electrodes due to equal distances from the positive electrode to the negative electrodes.

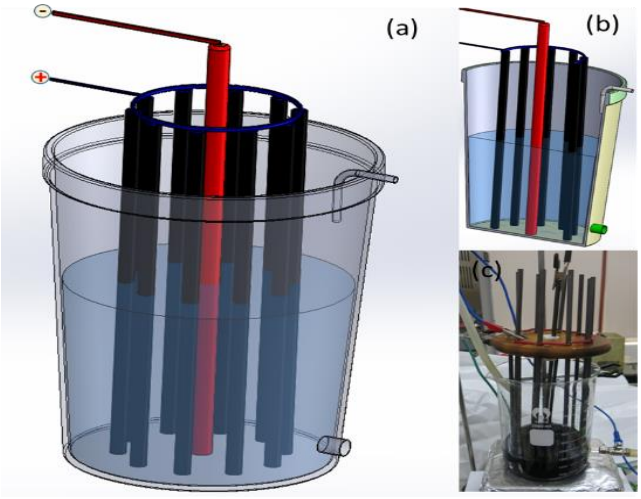

Figure 2.30 (a), (b) Experimental setup diagram and photo of the electrochemical system in the laboratory to manufacture O-MGSs material, (c) photo of the electrochemical system.

The results in Figure 3.31 show that the O-MGSs material has a thin layer similar to GSs, MGSs, with a material thickness of 3.2 nm determined from AFM measurements corresponding to a few layers of graphene. In addition, the Raman spectrum of O-MGSs also shows a symmetric 2D peak and a slight shift to a wavenumber of ~2700 cm-1 compared to HG at 2726 cm-1, indicating the formation of graphene [140]. Furthermore, the intensity ratio of the D band to the G band (ID/IG) is calculated to be 0.93 and 0.04 for O-MGSs and HG, as shown in Figure 3.32a. The higher ID/IG ratio of O-MGSs indicates a higher defect level compared to HG. Additionally, the XRD pattern of OGNs appears at 2θ ~ 26.0° with a broader peak width, corresponding to the (002) diffraction plane of graphite, compared to the sharp peak at the position 2θ ~ 26.6° of HG. It is noteworthy that the distance between the lattice planes of O-MGSs (0.342 nm) is larger than that of HG (0.334 nm), demonstrating that the electrochemical process has increased the distance between the layers in graphene.

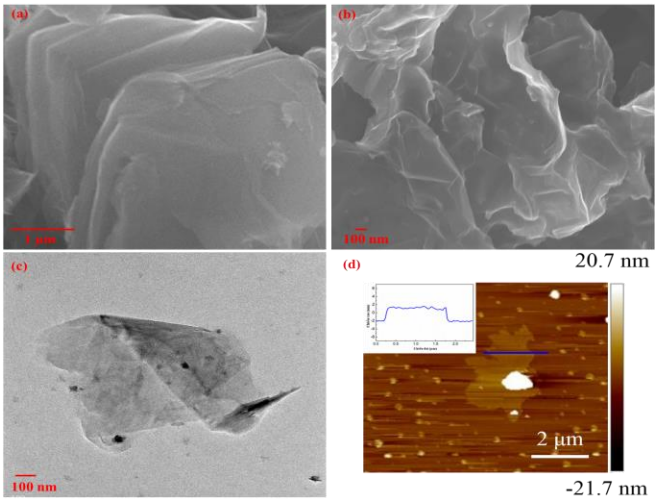

Figure 3.31 SEM images of (a) HG and (b) O-MGSs, (c) TEM and (d) AFM images of O-MGSs.

The XPS C1s analysis of O-MGSs in Figure 3.33 shows that the O-MGSs graphene sample has similar components to previous studies on GSs and MGSs, with many functional groups containing oxygen corresponding to binding energies at 285.6, 286.3, and 287.2 eV (C – OH, C – O, and C = O). The high-resolution O1s spectrum is also resolved into four peaks, corresponding to C = O (531.9 eV), C–O (532.7 eV), O–H (533.4 eV), and chemisorbed oxygen (534.3 eV). Specific calculations of the oxygen-carbon bond content in the sample from the C1s spectrum data (Table 3.7) show that the O-MGSs sample has a higher content than GSs and MGSs, approximately 25.31% compared to 16.47% and 19.29%, respectively.

Table 3.7 shows the bond content in the O-MGSs sample calculated based on the C1s spectrum data.

Sample	C=C (%)	C–C (%)	C–OH (%)	C–O (%)	C=O (%)
O-MGSs	46,23	28,23	17,99	6,23	1,09

The mechanism of the electrochemical exfoliation process in this study is depicted in Figure 3.34 and it's similar to what has been described in previous studies. In this research, a stable polarizing voltage of +30 V was applied, which is higher than in previous studies. The high voltage creates a strong electric field, leading to intense water electrolysis, resulting in numerous OH- groups, which may be the cause of the high oxygen content and defect density in O-MGSs.

i **3.3 Conclusion of chapter 3**

The electrochemical technology allows us to produce multi-layer graphene in one step, while functionalization of the material is proved by the following results:

- The GSs graphene material obtained by electrochemical technique using two conventional electrodes has the thickness of 3.5 nm which corresponds to about 4-6 layers with an ID/IG ratio of 0.79, relating to the attachment of oxygen-containing functional groups to the material. The synthesis conditions show that the electrolyte and polarizing voltage greatly affect on the morphology and structure of the obtained material.

- At a voltage of +60 V, the material obtained on the anode (A-GSs) is much thicker than the material obtained on the cathode (C-GSs) using a voltage of -60 V, and the carbon-oxygen bond ratio in the structure of A-GSs is also higher.

- The MGSs graphene material obtained by electrochemical technique using 10 pairs of electrodes with a scale mass achieves 10 g for each 60-minute reaction. The MGSs material has a thickness of 4 nm, a lateral size of about 2 µm, and a structural composition with many oxygen-containing functional groups which was confirmed through XPS spectra: -C = C at 284.5 eV, C – C bond at 285.7 eV, C-O/O – C = O/C = O bonds at positions 286.3, 288.7, and 287.2 eV with percentage ratios of 52.18, 28.53, 11.28, 5.74, and 2.27%, respectively.

- Improving the electrochemical technique using 10 positive electrodes arranged in a circle with a negative electrode at the center allows simultaneous

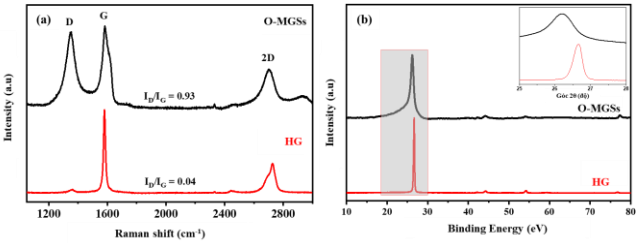

Figure 3.32 Raman spectrum (a) and XRD spectrum of HG and O-MGSs.

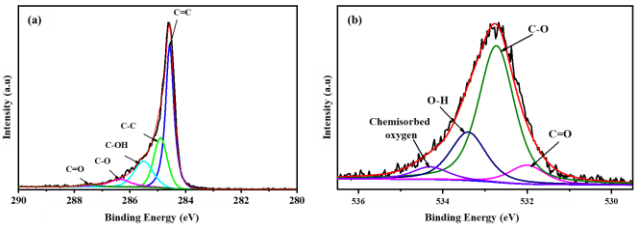

Figure 3.33 XPS spectra of (a) C 1s and (b) O 1s of O-MGSs.

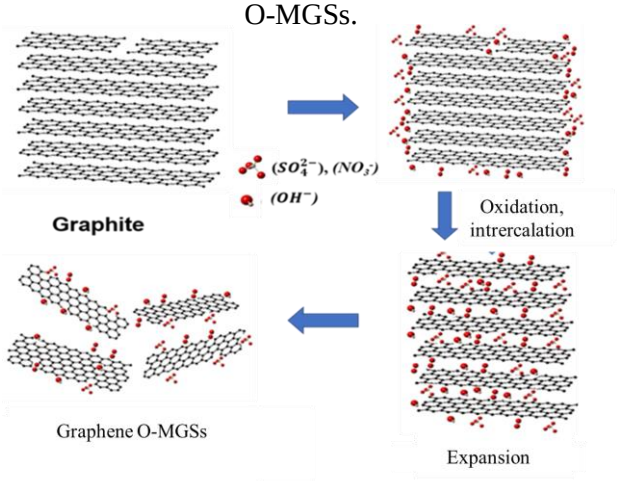

Figure 3.34. Schematic Illustration of the mechanism for producing O-MGSs graphene material from graphite using electrochemical methods.

functionalization in the same step to obtain O-MGSs material with a thin-layered morphology, a thickness of about 3.2 nm, a lateral surface size of 2 μm, and a structure containing plenty of oxygen suitable for adsorbent applications in environmental treatment.

Chapter 4. EXPERIMENTING THE ADSORPTION CAPACITY OF GRAPHENE MATERIALS SYNTHESIZED BY ELECTROCHEMICAL METHOD

The results obtained on material synthesis as being presented in chapter 3 of this thesis show that we can intentionally introduce oxygen-containing functional groups into the structure of graphene materials through electrochemical reactions. Enhancing the oxygen-containing functional groups on the material increases its dispersibility in solvents, which can facilitate the adsorption process of positively charged substances such as dyes or metal ions in water environments. The adsorption experiments in this dissertation only stopped at the experimental level to assess the potential application of the synthesized graphene materials as adsorbents. For this purpose, the dissertation only selected two materials, GSs (material synthesized using a two-electrode system) and O-MGSs (material with large-scale synthesis using a multi-electrode system) as adsorbent materials. Two common pollutants, methylene blue and arsenic metal ion As (III), were chosen as simulated water pollutants in the laboratory to evaluate the adsorption capacity of GSs and O-MGSs graphene materials. Factors that may affect the adsorption efficiency such as pH, adsorption time, initial MB concentration, material weight, and the content of oxygen-containing functional groups in the material were investigated.

4.1 Testing the adsorption capacity of GSs material

4.1.1 The isoelectric point of GSs material

4.1.2 The influence of pH of the solution

4.1.3 The influence of contact time

4.1.4 The influence of MB initial concentration

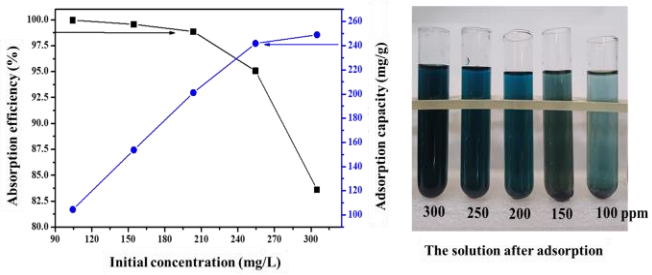

Figure 4.5 The dependence of adsorption efficiency on the initial concentration of MB.

The results show that under the same conditions and a specific material weight, as the concentration increases, the adsorption efficiency of MB onto the material decreases. At low MB concentrations in the solution, the adsorption sites on the GSs material may not be fully occupied due to an excess of available sites compared to the number of MB molecules, resulting in high efficiency. As the MB concentration increases and the material weight remains constant, there are not enough active sites on the adsorbent material surface to capture MB, leading to a decrease in adsorption efficiency.

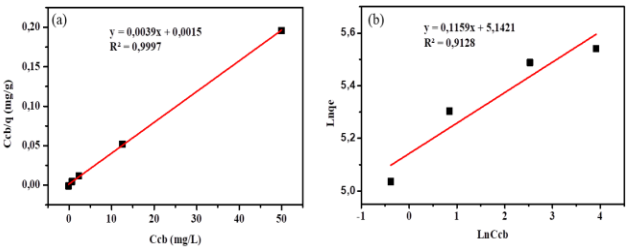

Figure 4.6 Isothermal model (a) Langmuir, (b) Freundlich

**** Isotherm adsorption mode***

To evaluate the MB adsorption process on the surface, we use two models, Langmuir and Freundlich, the results are shown in Figure 4.6 and table 4.2.

Table 4.2. Isothermal parameters of MB adsorption onto GSs

Langmuir Model				Freundlich Model		
q_{max} (mg/g)	K_L(L/mg)	R^2	R_L	n	K_F(L/g)	R^2
256,41	2,6	0,9997	0,28	8,63	171.07	0.9128

From Figure 4.6, it can be seen that the adsorption fits better with the Langmuir model with a higher correlation coefficient. This shows that the adsorption on the surface of GSs material is uniform. From the Langmuir isotherm model, we calculated the maximum adsorption capacity of MB on GSs material to be 256.41 mg/g, with the RL coefficient = 0.28 < 1, indicating favorable adsorption. In addition, according to the Freundlich isotherm model, we also obtained a value of n = 8.63, which falls within the range of 1-10, also indicating that the adsorption process is favorable.

Thus, it can be seen that the graphene GSs material has a good ability to adsorb MB with a maximum capacity of 256.41 mg/g under room temperature and neutral pH conditions. However, further research is still needed to improve the adsorption capacity of the obtained material.

4.1.5 The effect of functional groups on the efficiency of MB adsorption in water

As mentioned in the introduction, oxygen-containing functional groups are an important factor influencing the adsorption capacity of graphene materials. To verify this hypothesis, we selected a number of materials with different oxygen content to evaluate the influence of oxygen-containing functional groups on the MB adsorption capacity of the material. The selected material samples include GSs-k, GSs-sk, GSs-s, and the MB adsorption tests were conducted at different concentrations, with the results shown in Figures 4.7, 4.8, and Table 4.3. It can be observed that all three curves show a similar trend of decreasing performance as the initial MB concentration increases. With the same amount of material, the number of adsorption sites on the material surface (adsorption center) is fixed, while the increasing MB concentration in the solution leads to a higher residual MB amount in the solution, resulting in reduced treatment efficiency. According to Figure 4.7, with the same amount of material (0.02 g), a 60-minute adsorption time, and neutral pH, the MB adsorption efficiency increases in the order of materials: GSs-k, GSs-sk, and GSs-s.

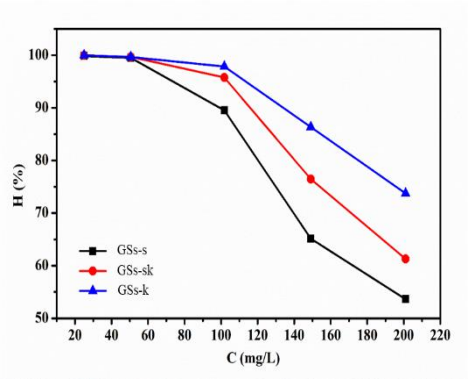

Figure 4.7 Adsorption efficiency of the samples depending on the initial MB concentration

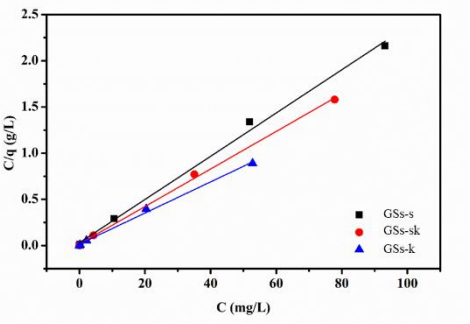

Figure 4.8 Langmuir isotherm diagram of MB adsorption onto the material

Processing the experimental results according to the linear Langmuir model, the maximum adsorption capacities of the GSs-k, GSs-sk, and GSs-s materials obtained are 270.27 mg/g, 303.03 mg/g, and 370.37 mg/g, respectively. The improved adsorption efficiency with increasing oxygen-containing functional groups content shows that these groups play an important role in enhancing the adsorption capacity of graphene materials. Therefore, enhancing the presence of oxygen-containing functional groups in the material composition is

essential for graphene materials in adsorption applications.

4.2 Application of O-MGSs materials for adsorption of MB and As (III) in water.

As presented in chapter 3, we have successfully fabricated O-MGSs materials on a gram scale. To evaluate the adsorption capacity of O-MGSs materials, the dissertation conducted experiments with simulated pollutants MB and As (III) in water. Similar to GSs materials, we continued to study the factors influencing the adsorption capacity of the materials, such as pH, time, and initial concentration of MB and As (III) in the solution. The results are presented in the following section below.

4.2.1 Point zero charge of O-MGSs materials

4.2.2 Adsorption of MB in water.

***4.2.2.1* Effect of pH**

***4.2.2.2* Effect of contact time**

4.2.2.3 Effect of initial concentration

In the initial concentration range investigated, when the initial concentration increases, the adsorption efficiency decreases and the adsorption capacity increases (Figure 4.13). This result can be explained similarly to the results of GSs adsorption of MB, which relates to the correlation between the number of adsorption sites and the amount of MB ions in the solution. We conducted a regression analysis of Ccb/q versus Ccb for the Langmuir model and lnqe versus lnCcb for the Freundlich model. The results we obtained are presented in Figure 4.14 and Table 4.5. The graph in Figure 4.14 shows the high correlation regression coefficients of both Langmuir and Freundlich models for MB adsorption, indicating the good fit of both models. In this case, the Langmuir model shows a higher fit with a coefficient R2 = 0.9974 and a coefficient RL = 0.0092 within the range of 0-1. Additionally, the coefficient n = 6.85 in the Freundlich model regression analysis also demonstrates the favorability of this adsorption process. The calculations according to this model are listed in Table 4.5, with a maximum adsorption capacity qmax = 476.19 mg/g. Comparing the adsorption efficiency of O-MGSs with other adsorbent materials previously published in studies (Table 4.6), it can be affirmed that the maximum adsorption capacity of O-MGSs is relatively high, showing the potential of O-MGSs in removing MB from wastewater. The maximum adsorption capacity for MB on O-MGSs increases compared to the adsorption on GSs, once again demonstrating that the oxygen-containing functional groups on

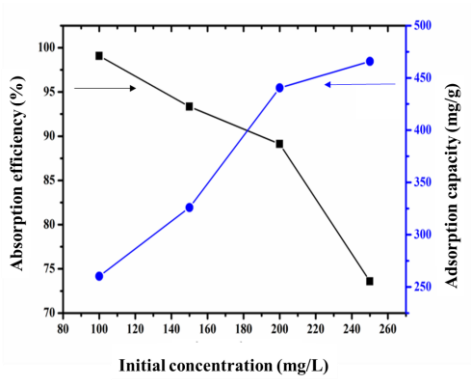

Figure 4.13 Effect of initial concentration on MB adsorption capacity on O-MGSs material.

Table 4.5 Isotherm parameters for MB and As adsorption onto O-MGSs.

Adsorbed substance	Langmuir isotherm model				Freundlich isotherm model		
	q_{max} (mg/g)	K_L(L/mg)	R^2	R_L	n	K_F(L/g)	R^2
MB	476,19	0,43	0,997	0,0092	6,85	265,28	0,9232

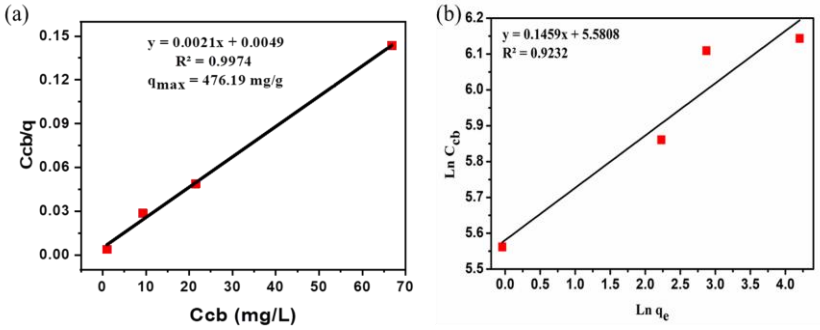

Figure 4.14. Langmuir (a), Freundlich (b) isotherm model of MB

the material play an important role in enhancing adsorption and better adsorption efficiency when the material contains multiple oxygen-containing functional groups.

4.2.3 Adsorption of As (III) in water.

In this study, we further expand to evaluate the adsorption capability of O-MGSs graphene material with heavy metal ion As (III) in water. Similar to the MB adsorption experiments in water, we continue to study the factors affecting the material's adsorption capacity, such as pH, time, and initial concentration of As (III) in the solution. The results are presented below:

***4.2.3.1* Effect of pH**

***4.2.3.2* Effect of contact time**

4.2.3.3 Effect of initial concentration

At the initial concentration range investigated, as the initial concentration increases, the adsorption efficiency decreases and the adsorption capacity increases (Figure 4.17). This result can be explained similarly to the MB adsorption results, which are related to the correlation between the number of adsorption sites and the amount of As (III) ions in the solution. In addition, the analysis based on the Langmuir and Freundlich isotherm models was applied, and the results obtained are presented in Figure 4.18 and Table 4.8. Figures 4.18a and b show the regression analysis of Ccb/q versus Ccb for the Langmuir model and ln qe versus ln Ccb for the Freundlich model for the adsorption of As (III) onto O-MGSs material. It can be seen that for the adsorption of As (III), the Freundlich model is more suitable with a higher regression coefficient R2 = 0.9925.

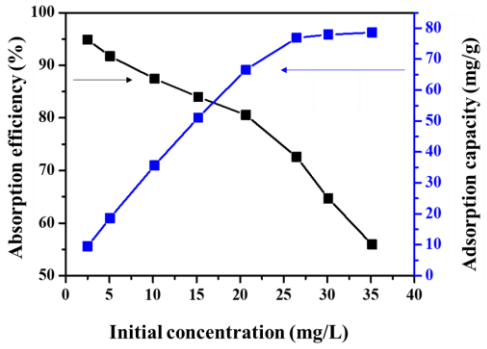

Figure 4.17 Effect of initial concentration on As (III) adsorption capacity on O-MGSs material.

Table 4.8 Isothermal parameters of As(III) adsorption onto O-MGS

Adsorbed substance	Langmuir isotherm model				Freundlich isotherm model		
	q_{max} (mg/g)	K_L(L/mg)	R^2	R_L	n	K_F(L/g)	R^2
As (III)	93,45	0,60	0,9842	0,0272	1,86	29,81	0,9925

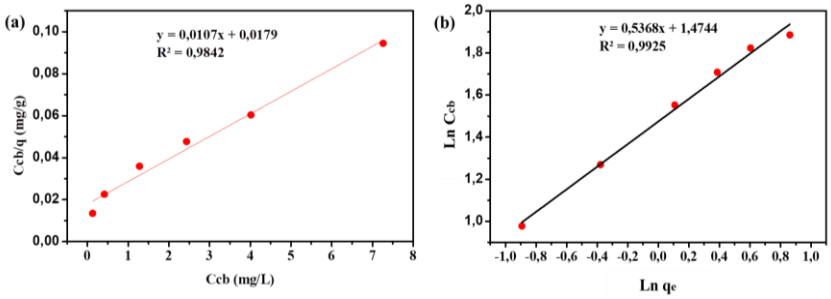

Figure 4.18. Langmuir (c), Freundlich (d) isotherm model of As(III).

The maximum adsorption capacity qmax = 93.45 mg/g was calculated according to the Langmuir model. Comparing the adsorption efficiency of O-MGSs with other adsorbent materials reported in previous studies (Table 4.9), it can be affirmed that the maximum adsorption capacity of O-MGSs material is relatively high, demonstrating the potential of O-MGSs material in removing As (III) from water. The O-MGSs material has a good adsorption capacity for As (III), showing potential for removing heavy metals from water.

4.3 Evaluate the reusability of graphene materials.

The evaluation results of the desorption process are presented in Figure 4.19.

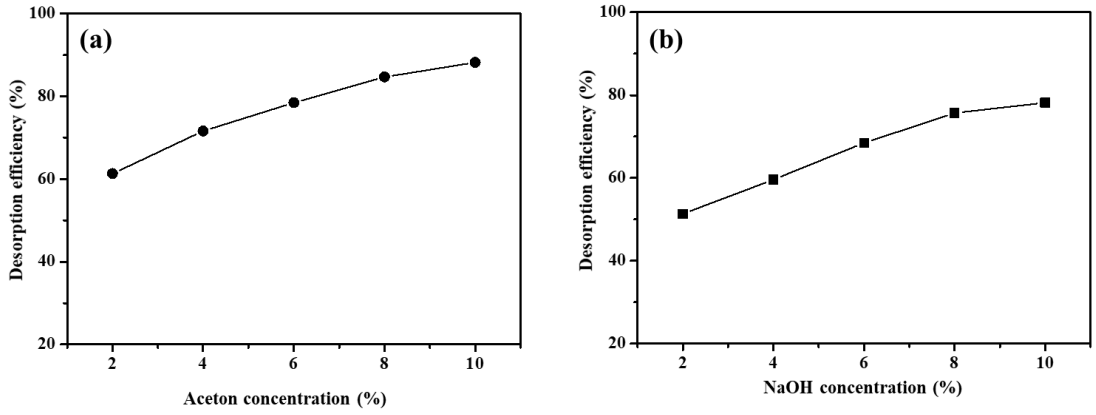

Figure 4.19 Desorption efficiency (a) of MB using acetone and (b) of As (III) using NaOH

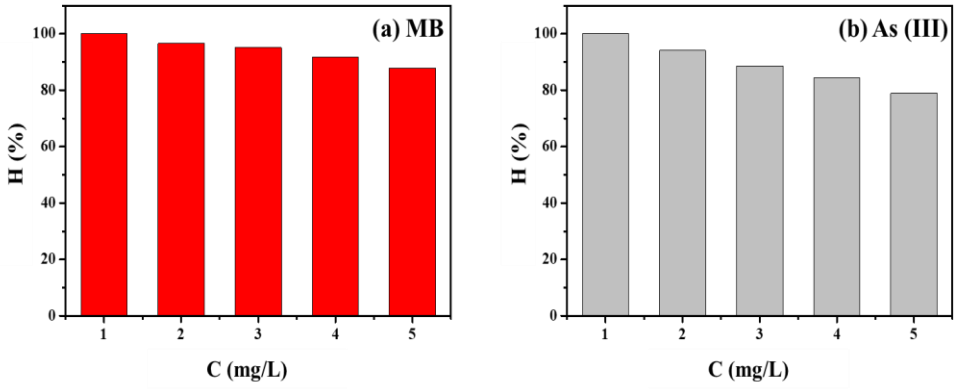

Figure 4.20 Adsorption efficiency (a) of MB and (b) of As (III) on O-MGSs material. according to the material regeneration cycle.

The material is regenerated and then subjected to adsorption experiments with two pollutants, MB and As (III), to assess reusability. The experimental results are presented in Figure 4.20. It can be seen that the removal efficiency decreases over cycles. Specifically, the adsorption efficiency achieved in the first reuse is 97.31% for MB and 62% for As (III), which gradually decreases to 86.85% for MB and 48.92% for As (III) in the fifth test. The reason for the decrease in efficiency is that the material cannot be completely regenerated after use, or some adsorption sites are gradually lost after cycles. The results obtained after multiple reuses demonstrate the feasibility of regenerating O-MGSs material for multiple uses.

4.4 Conclusion of chapter 4

The research evaluating the adsorption capacity of GSs and O-MGSs materials shows:

- Graphene GSs material has favorable adsorption capacity for MB. The isothermal adsorption process of GSs samples fits well with the Langmuir isotherm model, and the adsorption kinetics follow a pseudo-second-order kinetic model. According to the Langmuir isotherm model, the maximum adsorption capacity of GSs material for MB is 256.41 mg/g.

- The presence of oxygen-containing functional groups on the material significantly affects its adsorption capacity, as demonstrated by the increasing maximum adsorption capacity for MB of GSs-k, GSs-sk, and GSs-s materials, which are 270.27, 303.03, and 370.37 mg/g, respectively.

- Functionalized graphene material (O-MGSs) with thin-layered morphology, a thickness of about 3.2 nm, a lateral size of 2 μm, and a structure containing abundant oxygen, exhibits good adsorption capacity for MB and As (III) with maximum adsorption capacities of 476.19 mg/g and 93.45 mg/g, respectively.

CONCLUSION

- The electrolytic dissolution process has been established to produce multi-layer graphene materials while functionalization of the material surface with oxygen-containing functional groups, allowing for application as an adsorbent to remove MB dyes and As metals in water.

- The graphene GSs material which was obtained by electrolysis technique using two electrodes, electrolyte containing KOH + (NH4)2SO4, voltage of +10 V has a thickness of 3.5 nm, corresponding to about 4-6 layers with an ID/IG ratio of 0.79 relating to the attachment of oxygen-containing functional groups to the material.

- An electrolytic system with high automation capability has been established using 10 electrodes, electrolyte containing KOH + (NH4)2SO4, and a voltage of +15 V to produce multi-layer graphene material MGSs with a yield of 10 g per reaction for 60 minutes. The MGSs material has a thickness of 4 nm, a surface size of 2 μm, and a structural composition containing numerous oxygen-containing functional groups confirmed through XPS spectra: -C = C at 284.5 eV, C – C bond at 285.7 eV, C-O/O – C = O/C = O bonds at positions 286.3, 288.7, and 287.2 eV with percentage ratios of 52.18, 28.53, 11.28, 5.74, and 2.27%, respectively.

- The oxygen-containing functional groups are intentionally introduced in the electrochemical exfoliation process using a 10-anode and 1-cathode electrochemical system, an electrolyte containing a mixture of KOH + (NH4)2SO4 + NH4NO3, and a voltage of +30 V. This process produces graphene material (O-MGSs) with a thin-layered morphology, a thickness of 3.2 nm, a lateral surface size of 2 μm, and a structure containing abundant oxygen, enabling high adsorption capacity for MB and As (III) with maximum adsorption capacities of 476.19 mg/g and 93.45 mg/g. The advantage of this technique is its high level of automation in a single step, using readily available water as the solvent for equipment and electrolyte, facilitating scalability.

- The evaluation of material reusability was conducted on O-MGSs samples, showing that O-MGSs material has an adsorption efficiency of 86.85% for MB and 48.92% for As (III) after 4 reuse cycles.

- The thesis results demonstrate that the electrochemical technique allows for the large-scale production of multilayer graphene material, meeting the material demands for environmental treatment and other applications.

LIST OF THE PUBLICATIONS RELATED TO THE DISSERTATION

1. Pham Van Hao, Phan Ngoc Minh, Phan Ngoc Hong, Nguyen Nhat Huy, Phung Thi Oanh, Hai Thanh Nguyen, Trang Doan Tran, Dang Van Thanh, Van Thi Khanh Nguyen and Nguyen Van Dang, *Gram-scale synthesis of electrochemically oxygenated graphene nanosheets for removal of methylene blue from aqueous solution*, **Nanotechnology**, 2021, Volume 32, Issue 16, Pages 16LT01.

2. Ha Xuan Linh, Phung Thi Oanh, Nguyen Nhat Huy, **Pham Van Hao,** Phan Ngoc Minh, Phan Ngoc Hong, Dang Van Thanh, *Electrochemical mass production of graphene nanosheets for arsenic removal from aqueous solutions*, **Materials Letters**, 2019, Volume 250, Pages 16-19.

3. **Pham Van Hao,** Ha Xuan Linh, Phung Thi Oanh, Phan Ngoc Hong, Nguyen Nhat Huy, Dang Van Thanh, Nguyen Van Dang, *Effect of synthesis conditions on methylene blue adsorption capacity of electrochemically preparated graphene,* **Vietnam Journal of Catalysis and Adsorption**, 2020, 9-issue 3, Pages 9-14.

4. **Pham Van Hao,** Ha Xuan Linh, Phung Thi Oanh, Phan Ngoc Hong, Nguyen Nhat Huy, Dang Van Thanh, *A study on the effectiveness of polarization conditions on the morphology and structural properties of graphene preparating by plasma electrochemical method,* **Vietnam Journal of Chemistry**, 2017, Volume 55, 3e12, Pages 341-345.

5. **Pham Van Hao**, Ha Xuan Linh, Nguyen Thi Kim Ngan, Phan Ngoc Hong, Nguyen Thi Thuy, Nguyen Nhat Huy, Phung Thi Oanh, Dang Van Thanh, *Arsenic removal from aqueous solutions by graphene nanosheets prepared from electrochemical exfoliation of graphite rod,* **the 6th international workshop on nanotechnology and application** - iwna 2017, 2017, amn-035-p Pages 577 – 581.